J. Micromech. Microeng. **17** (2007) 722–729 doi:10.1088/0960-1317/17/4/008

Fabrication of a LCP-based conductivity cell and resistive temperature device via PCB MEMS technology

Heather A Broadbent, Stanislav Z Ivanov and David P Fries

Ecosystems Technology Group, College of Marine Science, University of South Florida, St Petersburg, FL 33704, USA

E-mail: heather@marine.usf.edu

Received 8 January 2007, in final form 11 February 2007
Published 8 March 2007
Online at stacks.iop.org/JMM/17/722

Abstract

Printed circuit board microelectromechanical systems are a set of fabrication techniques that use traditional inexpensive printed circuit board processes to construct microsensors. These techniques keep gaining popularity and are utilized herein. The design, fabrication and construction of a miniature, low-cost conductivity cell and resistive temperature device transducers are presented. The transducers utilize a liquid crystal polymer (LCP), a thin-film material, which exhibits moisture resistant properties that makes it suitable for aquatic applications. Novel processing techniques that are reported here include the use of a direct-write photolithography tool eliminating the use of photomasks and chemical catalytic metallization of LCP material. The rapid fabrication of these devices and the repeatability of the fabrication are demonstrated by comparing the calibration of multiple devices. The sensors' sensitivities are found to be 1082.40 ± 144.18 mS cm^{-1} per siemens and 5.910 ± 0.765 °C per ohm for the conductivity and temperature transducers, respectively.

(Some figures in this article are in colour only in the electronic version)

1. Introduction

1.1. Recent trend of using PCB MEMS coupled with LCP

There has been considerable interest in the development of microelectromechanical systems (MEMS) fabricated using printed circuit board (PCB) processes combined with non-standard polymer materials such as liquid crystal polymer (LCP). Printed circuit board fabrication processes offer rapid development cycles and inexpensive mass production of microsensors. This is due to the lower cost of materials and equipment compared to traditional silicon or ceramic MEMS technology. Merkel *et al* demonstrated the use of PCB technology to develop a polyimide pressure sensor [1].

LCP material exhibits a combination of electrical, thermal, mechanical and chemical properties that other polymers do not. LCP is a thermoplastic dielectric material developed specifically for single layer and multilayer substrate constructions with unique structural and physical properties. LCP material is characterized by low and stable dielectric constant and dielectric loss (0.004) [2]. LCP has good dimensional stability and low modulus, allowing it to bend easily for flex and contour applications. LCP has extremely low moisture absorption (0.04%) and low moisture permeability, which allows the material to maintain stable electrical, mechanical and dimensional properties in humid environments. LCP has very high chemical resistance and is unaffected by most acids, bases and solvents [3]. The combination of these physical properties make LCP material well suited for underwater sensor applications. Wang *et al* demonstrated the development of LCP-based flow sensors and tactile sensors micromachined using PCB MEMS fabrication processes [4].

1.2. Maskless photolithography tool

The maskless photolithographic patterning tool technology utilizes reflective micro-optics in combination with mixing and imaging lenses to allow direct circuit image projection

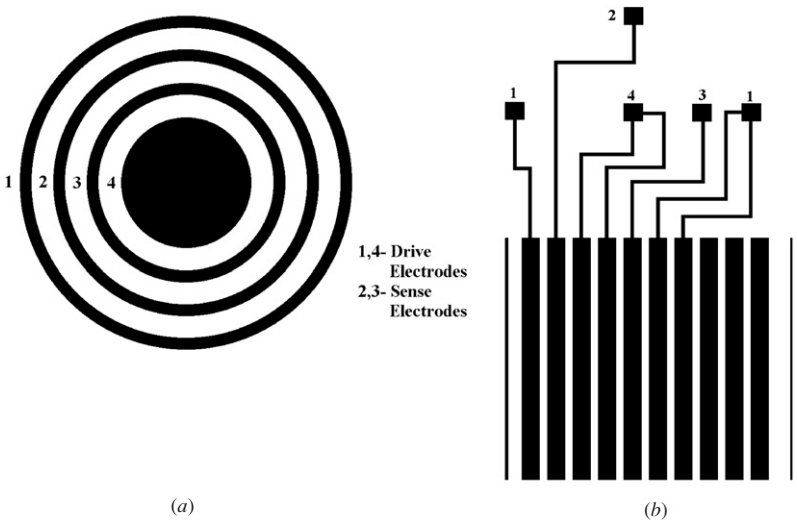

Figure 1. The conductivity cell artwork used with the maskless photolithography tool. (*a*) The four-electrode ring top layer. (*b*) Conductive pads and fingers bottom layer.

onto a substrate surface. In this technique, reflective microoptoelectromechanical (MOEM) elements are used to spatially modulate light such that light can be controlled on the several micron-sized regime, simultaneously over a 13 mm × 10 mm sized field of view. The desired pattern is designed and stored using conventional computer-aided drawing tools and is used to control the positioning of the individual elements in the spatial light modulator to reflect the corresponding desired pattern. In addition, an automated stage with 6 inch × 6 inch travel has been incorporated with the system to allow for stitching of larger patterns on a substrate, while maintaining a small feature size. The stage is capable of movement in the *X*, *Y*, *Z* and theta directions with a stepping resolution of 1 μm [5].

This patterning tool, by eliminating the use of traditional contact photomasks, provides distinct photolithographic advantages over conventional methods. Once the pattern has been designed using the desired software, it can be changed and manipulated in much less time than required to generate a traditional photomask. Pattern changes can be performed from seconds to minutes. This allows for rapid generation of numerous prototypes. Traditional photomasks must be filled and stored in a clean, temperature and humidity-controlled environment. The patterns generated for the maskless tool are electronically stored in a memory file on a computer, thus eliminating mask contamination and the need for proper storage space. The maskless photolithographic tool eliminates the need for photomask generating tools such as cameras, printers and harsh chemicals, along with the separate UV exposure unit. Low cost microsensors and microsystems can be fabricated rapidly by using the novel maskless photolithographic tool [6].

1.3. Aquatic sensors

Conductivity and temperature are fundamental properties of marine and fresh waters from which salinity and density can be derived and are commonly used in the monitoring and analysis of marine and freshwater environments, industrial wastewater, municipal wastewater and desalination plant effluent [7]. Based on the requests from both oceanographic and environmental monitoring applications, miniature, expendable, reliable and cost-effective sensors for measuring conductivity and temperature are in high demand. Some oceanographers and biologists have experimented with the use of animals as vehicles for the remote collection of information [8]. However, limitations in sensor size and resolution have made it difficult to collect adequate data using this method [9]. Research efforts have been focused on an autonomous expendable conductivity, temperature and pressure (CTD) profiler for ocean data collection [10].

In the past, planar conductivity sensors have been fabricated using alumina or quartz glass substrates. Farrugia and Fraser have used a multi-layer screening technique for fabrication of a conductivity cell using alumina [11]. Norlin *et al* used micromachining and MEMS techniques for fabrication of planar Pt conductivity electrodes and Pt thermistors using a quartz glass wafer [12]. In this work, novel LCP material combined with a novel photolithography tool is used to fabricate the PCB MEMS-based conductivity and temperature sensors. LCP is a thermoplastic material that exhibits distinctive physical properties. The advantages of LCP include low moisture absorption, high chemical resistance and mechanical flexibility [13]. This paper describes the design and microfabrication processes developed to construct the LCP-based conductivity and temperature sensors. Future work will be the in-depth optimization and characterization of each transducer.

2. Theoretical considerations

2.1. LCP planar four-electrode conductivity cell

The conductivity cell was constructed using electroless nickel–gold–platinum black metals plated on 8 mil thick LCP material. As shown in figure 1(*a*), the cell is of planar and circular geometry such that all the current between the two drive electrodes (rings 1 and 4) passes over the sense electrodes (rings 2 and 3). The double-sided, planar design simplifies

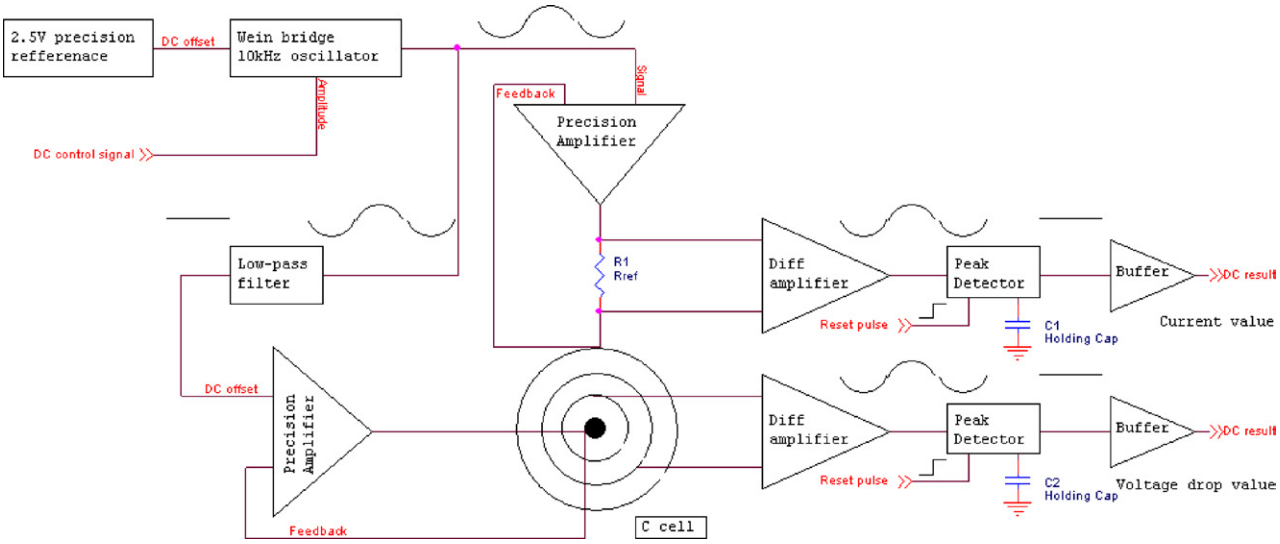

Figure 2. Schematic of the conductivity circuit.

the manufacturing of the cell as there is no closed volume consideration, a characteristic which also helps to limit biofouling; the primary current path is limited to ∼1 mm above the electrodes, which makes the packaging compact. The circular design also enables directionless flow profiles to be measured easily and without additional calibration. Typical cell dimensions are 10 mm diameter.

In the final fabricated sensor, the exposed conductive rings of figure 1(*a*) are connected to the pads correspondingly numbered in figure 1(*b*), with plated through-holes drilled before the plating phase of the fabrication process. The pattern of figure 1(*b*) is used as a drilling template which is subsequently used to align the top and bottom layers of the sensor for the metallization process. Ten long fingers are used to interface to a standard 10 pin folded flex cable (FFC) connector that interfaces to the electronics on a standard PCB. The LCP material high mechanical strength allows the use of such a pressure contact, avoiding soldering and/or bonding techniques, which can be expensive and damaging to the sensors by introducing additional heat and chemistry to the fabrication process.

Conductivity of the cell is determined by measuring the voltage developed between the two sense electrodes when a known current is applied through the drive electrodes and the known cell constant (K factor) of the sensor. The determination of conductivity is derived from the formula

$$Ck = I/E^*L/S, \tag{1}$$

where I is the electrical current measured through the cell, E is the voltage used to bias the cell, L is the length between the voltage measuring electrodes, S is the mean contact area of the current-carrying electrodes and L/S is the K factor.

The four-electrode design is desired to obtain accurate measurements. The bias potential as applied to the external drive electrodes and the current is thus measured through the drive amplifier (figure 2). Using the known cell constant (K factor), the known bias voltage and the resulting current can be used to calculate the conductivity measurement when the cell is undamaged. A differential amplifier between the two intermediate electrodes provides the potential drop between them, which can also be used for the conductivity measurement by replacing the known bias voltage and the resulting smaller cell constant. Since the electrodes are attached to the high impedance input of the amplifier, only the input bias current flows through the electrodes, which is not enough to induce corrosion. Therefore, the cell constant between the sense electrodes, fixed by the cell geometry, can only be changed through biofouling, affecting their shape, contact surface and area. The extent of the cell damage can thus be easily measured by comparing the drive electrode bias reading to the sense electrode voltage drop.

2.2. LCP resistive temperature device

The temperature sensor designed is a resistive temperature device (RTD), which is a thin-film metallic circuit that exhibits a linear change in resistance with change in temperature. The electrical resistance of the conductor at any temperature can be calculated by using the formula

$$R_T = R_r(1 + \alpha(T - T_r), \tag{2}$$

where R_T is the resistance of conductor at temperature (T), R_r is the resistance of conductor at reference temperature (T_r) and α is the temperature coefficient of resistance at reference temperature.

The four-electrode design was used for accurate measurements of the RTD. The sensor was biased with a constant current source formed by a drive amplifier and a known sense resistor; the voltage drop across the sense resistor, which was connected in series with the sensor, was regulated by the amplifier. The voltage drop developed by the RTD was measured by a differential amplifier with high input impedance. The resistance of the sensor can be calculated by this formula

$$R_T = V/I, \tag{3}$$

where R_T is the resistance of the conductor at temperature (T), V is the voltage drop across the sensor and I is the applied bias current.

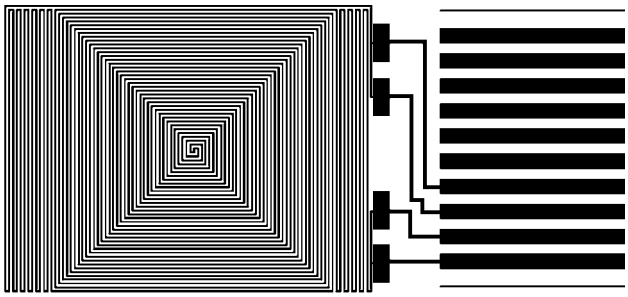

Figure 3. The temperature sensor artwork used with the maskless photolithography tool.

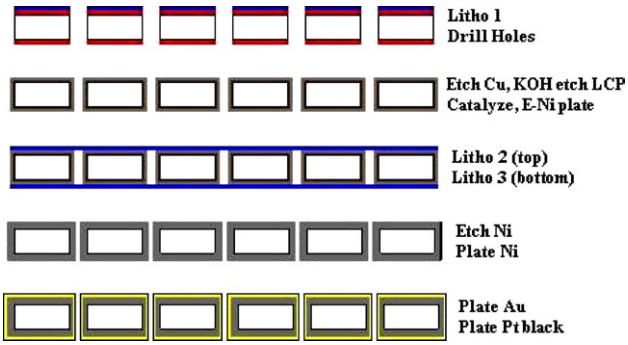

Figure 4. Schematic illustration of the process sequence for the conductivity cell.

The fabricated sensor has a concentric design that consists of two parallel traces with 90° angles that meet in the center (figure 3). The 90° angles of the design reduce inductance (orthogonal fields), the side traces have varying lengths so that they do not resonate at a particular frequency and the side-by-side traces reduce noise. The design is quite long (∼106 cm) with thin trace widths (∼37 μm) to provide greater sensitivity. The design exhibits maximum packing density within a small area (13 mm × 10 mm) and the use of LCP material enables the sensor to be flexible or rigid, depending on the thickness.

The sensor was fabricated with 6 mil thick copper-clad LCP material using PCB MEMS microfabrication processes coupled with the maskless photolithography tool. Copper was chosen as the base metal because it exhibited linear results over the desired water temperature range (−5 to 65 °C), it limited bi-metal junctions and was cost effective because it was pre-clad on the LCP material.

3. Development of novel PCB MEMS fabrication processes for LCP sensors

The conductivity cell was fabricated using PCB/MEMS techniques combined with the maskless photolithographic tool and 8 mil thick Cu-clad liquid crystal polymer material. An overview of the process sequence is shown in figure 4.

First, the conductivity cell contact pad artwork was patterned on the LCP material using the photolithographic tool. This pattern was then used as a template to drill the through-holes. Once the through-holes were drilled, the copper was entirely etched and the LCP was micro-etched to roughen the surface for metallization [14]. After the micro-etch, the surface

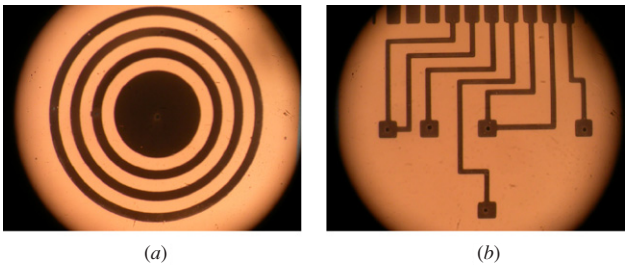

(*a*) (*b*)

Figure 5. Photos of the top (*a*) and bottom (*b*) layers of a microfabricated conductivity cell.

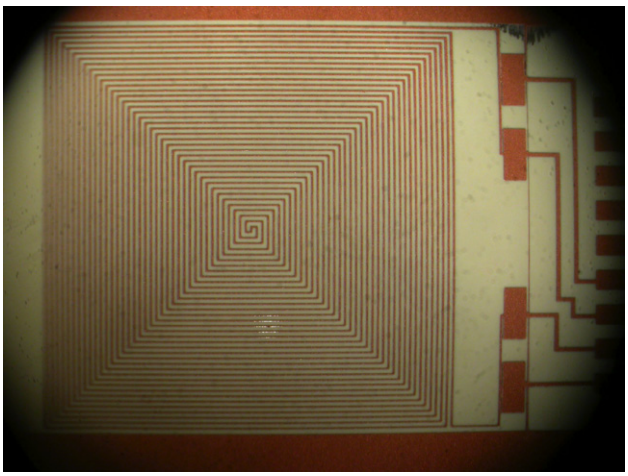

Figure 6. Photo of the microfabricated copper resistive temperature device.

of the etched LCP material was examined and measured against the surface of a non-etched piece of LCP using a Veeco Wyco NT 3300 Optical. The Ra measurements resulted in a difference in surface area from 913.80 nm (before micro-etch) to 955.88 nm (after micro-etch). The images produced show a change in surface topography where the etched piece has a rougher surface compared to the non-micro-etched piece. Also the LCP thickness was measured before (0.008 45 inch) and after (0.007 90 inch) the micro-etch resulting in a 0.000 55 inch loss of surface material. The LCP substrate was then catalyzed for metallization and subsequently plated with a thin film (0.4 μm) of electroless nickel. The conductivity electrode cell was patterned onto the thin LCP/nickel substrate. The conductivity cell pattern was redeposited with a 25 μm thick layer of electroless nickel. Once the nickel metal was built up, a thin layer of gold was chemically deposited. After fabrication, the conductivity cell pads and leads (figure 5(*b*)) were coated with a thermal shock resistant conformal coating to prevent seawater corrosion. Then a layer of porous platinum black was electroplated to the surface of the conductivity rings [15, 16].

As with the conductivity cell, the temperature sensor was fabricated using PCB MEMS techniques, the maskless photolithographic tool and 6 mil thick Cu-clad LCP material. The RTD was patterned on the copper-clad LCP substrate and then the copper was chemically etched away (figure 6). The average measured trace width of the RTD is 37 μm. Then the temperature sensor was plated with electroless tin to protect it from oxidation.

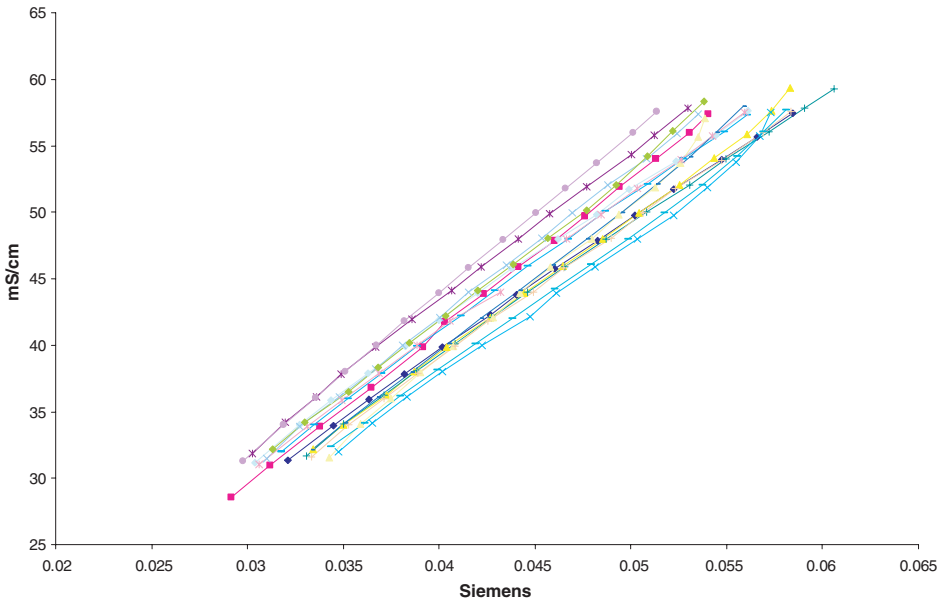

Figure 7. Calibration curve graph of 17 conductivity cells fabricated.

4. Results and discussion

4.1. Microsensor reproducibility via microfabrication

In order to test the reproducibility of the PCB MEMS fabrication process, multiple conductivity and temperature sensors were constructed. After microfabrication the sensors were individually calibrated and linear regressions were performed on the data. Seventeen conductivity cells were calibrated using International Association for the Physical Sciences of the Oceans (IAPSO) standard seawater samples (Ocean Scientific International Limited, Hamshire, UK). The conductivity calibration procedure entailed taking consecutive measurements of the standard's conductivity while varying the temperature of the solution. It is known that a solution's conductivity is a function of temperature, and there is a mathematical expression that relates these two variables. The conductivity cell was submersed with a platinum resistive temperature device in a beaker of 34.995 salinity sample and heated to 32 °C using a water bath. Once the sample stabilized at the chosen bath temperature, a conductance reading (in siemens) was taken. Temperature readings from the sample were taken to verify actual solution temperature. The temperature of the water bath was reduced by 2 °C increments and measurements were acquired from 32 to 4 °C. Five conductance measurements were recorded and averaged to obtain a stable reading at every given temperature. The conductivity (mS cm^{-1}) of the standard seawater sample (34.995) per temperature was calculated using the Practical Salinity Scale 1978 [17]. The formula states

$$S = a_0 + a_1 R_t^{1/2} + a_2 R_t + a_3 R_t^{3/2} + a_4 R_t^2 + a_5 R_t^{5/2} + \Delta S, \quad (4)$$

where ΔS is given by

$$\Delta S = [t - 15/1 + 0.0162(t - 15)] \times \left(b_0 + b_1 R_t^{1/2} + b_2 R_t + b_3 R_t^{3/2} + b_4 R_t^2 + b_5 R_t^{5/2}\right),$$

and

$$a_0 = 0.0080 \qquad b_0 = 0.0005$$
$$a_1 = -0.1692 \qquad b_1 = -0.0056$$
$$a_2 = 25.3851 \qquad b_2 = -0.0066$$
$$a_3 = 14.0941 \qquad b_3 = -0.0375$$
$$a_4 = -7.0261 \qquad b_4 = 0.0636$$
$$a_5 = 2.7081 \qquad b_5 = -0.0144$$

valid from $S = 2$ to 42, where

$$R = C(\text{sample at } t)/C(\text{KCl solution at } t).$$

The conductance (siemens) of the conductivity cell was plotted against the calculated conductivity (mS cm^{-1}) (figure 7). As the conductance is a linear function of the conductivity, linear curve parameters were regressed using the method of least squares. The slopes were then averaged and a sensitivity of 1082.40 mS cm^{-1} per siemens with a standard deviation of ±144.18 was determined. The average coefficient of determination ($R^2 = 0.999$) indicates excellent linear correlation between the measured (conductance) and predicted variable (conductivity) for all the LCP-based conductivity cells fabricated using PCB MEMS technology.

Eleven resistive temperature devices were calibrated using DI water in a temperature-controlled water bath. The sensor was submersed in a 200 ml beaker along with a calibrated platinum resistive temperature device. Once the DI water stabilized at the desired water bath temperature, the resistance (Ω) measurement along with the temperature measurement from the calibrated platinum RTD was recorded. Five resistance measurements were averaged to obtain a stable reading at each temperature. The resistance (Ω) of the temperature sensor was plotted against the temperature (°C) (figure 8). Linear regression lines were calculated for each sensor along with the coefficient of determinations. The slopes

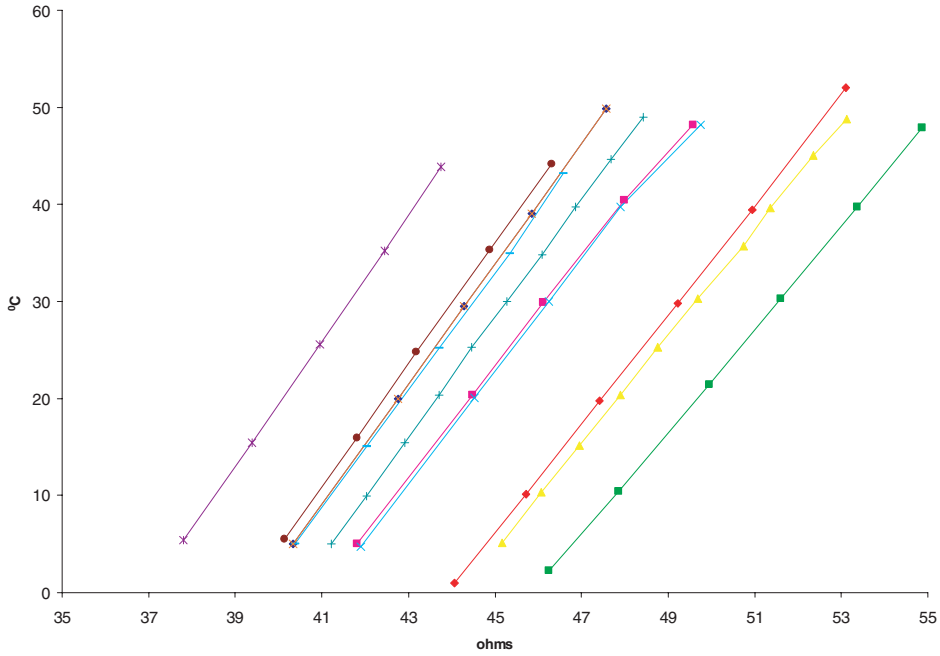

Figure 8. Calibration curve graph of 11 RTDs fabricated.

were then averaged and a sensitivity of 5.910 ± 0.765 °C per ohm was determined. The calculated average R^2 value (1.000) indicates excellent linear correlation between the measured (resistance) and predicted variable (temperature) for all the LCP-based RTD transducers fabricated using PCB MEMS technology.

4.2. Comparisons of conventional probes

The LCP PCB MEMS-based conductivity cell was tested against a carbon four-pole conductivity probe (Mettler Toledo Inlab 730). The conventional conductivity probe was calibrated using a standard of 12.88 mS cm^{-1}. Conductivity standards (KCl) were used to perform the test. The standards used were 2000, 5000, 7000, 10 000, 12 880, 15 000, 20 000, 30 000, 40 000, 50 000, 60 000 and 70 000 μMHOS @ 25 °C respectively. Both sensors were submersed in the standard sample along with a RTD, and measurements were acquired after a 1 min acclimation period. The conventional conductivity probe is equipped with a temperature sensor, which automatically calculates the temperature compensation for the conductivity measurement. Temperature measurements for each standard were recorded using the submerged RTD. The conductivity measurement taken from the LCP-fabricated cell was corrected using the temperature compensation formula

$$R/1 + 0.019(T - 25),$$

where R is the measured mS cm^{-1} reading and T is the measured temperature.

The temperature-compensated conductivity values were then plotted against the commercial probe measurements and the sample regression equation and R^2 were calculated. The slope of the best-fit regression line indicates a 3% deviation of the straight line. Figure 9 shows an adequate correlation

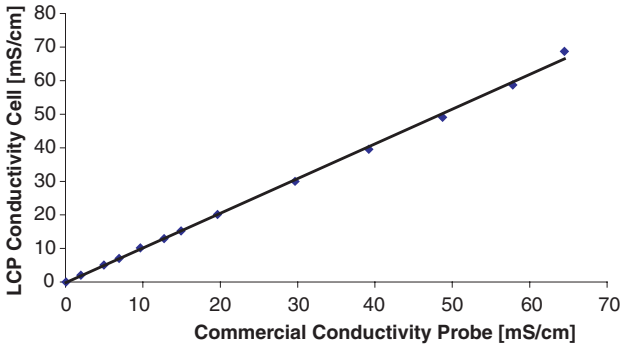

Figure 9. Conventional conductivity probe versus LCP-fabricated conductivity cell.

of the two sensors up to 50 mS cm^{-1}. The differences calculated between the conductivity cell and the commercial probe were approximately 3% for each conductivity value. The differences show that even though the fabricated sensor performance is a function of the measured range, it performs relatively well until the upper limit (70 mS cm^{-1}) was reached.

The LCP-based RTD sensor was tested against a commercial temperature probe (Fluke 80T-1500 temperature adapter). Both sensors were submersed in a beaker of deionized water and heated to a specific temperature using a recirculating water bath. The temperature devices were measured from 50 °C to 10 °C in increments of 5 °C. The R^2 value (0.9997) shows good linear correlation between the LCP RTD and the commercial temperature probe. The regression coefficient or slope (0.9917) of the compared sensors was close to 1.0000. Figure 10 is the temperature comparison data of both sensors plotted against the known temperature of the water bath. The differences between the RTD and the conventional probe range from −0.64 to 0.15 °C.

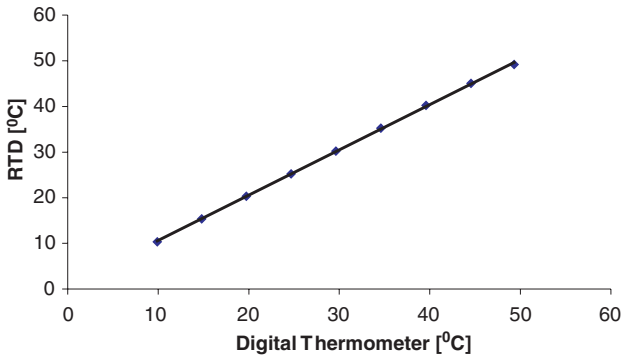

Figure 10. Conventional digital thermometer versus LCP-fabricated RTD.

4.3. Potential LCP-microsensor resolutions

In order to obtain an estimate of the resolution of the fabricated sensors, all voltages were measured by a differential sigma-delta ADC with a 24 bit resolution. The signed conversion with a 2.50 volts reference results in a 298 nano-volt resolution.

The conductivity sensor was biased by a constant voltage amplitude sinusoidal waveform at 10 kHz. The current supplied to the cell to maintain the signal was measured through a series reference resistor. The ADC measures the voltage drop across R_{ref} differentially. The calculation of the current bias through the cell therefore yields 19.9 nano-amps resolution, which when used with a 300 mV bias, yields 66.3 nano-siemens resolution. A linear regression curve was then applied to the conductance measurement consisting of a gain (average sensor sensitivity) and an offset term that can be used to determine the conductivity resolution; by multiplying the gain (1082.40 mS/cm/S) with the conductance resolution, a conductivity resolution of 0.000 718 mS cm^{-1} was obtained.

The resistive temperature device was biased by a programmable current source. The current source uses a reference resistor in series with the sensor and the power amplifier to set the current by adjusting the voltage bias across R_{ref}. The usual voltage bias that produces the most gain was 2.50 V, which sets the circuit to 250 μA with 10.0 kΩ R_{ref}. The ADC measures the voltage drop across the sensor differentially; thus the calculation for the resistive resolutions yields 1.19 mΩ. A linear regression curve was then applied to the resistive calculation result consisting of a gain (average sensor sensitivity) and offset term that can be used to determine the temperature resolution; by multiplying the gain (5.91 °C Ω^{-1}) with the resistance resolution, we obtained a 0.007 03 °C potential temperature resolution.

5. Conclusions

The microfabrication of LCP-based electrode cell conductivity sensors and resistive temperature devices has been demonstrated. It has been shown that the manufacture of the MEMS transducers in a PCB format is rapid and direct using a novel maskless photolithographic-based process. The above experimental data have verified that the conductivity and temperature transducers perform as intended with sensitivities of 1082.40 ± 144.18 mS cm^{-1} per siemens and 5.910 ± 0.765 °C per ohm, respectively. Further experiments have verified that the conductivity and temperature sensors are comparable with conventional sensors/probes, and a potential resolution of 0.000 718 mS cm^{-1} and 0.007 03 °C respectively were obtained. The novel PCB MEMS fabrication technique used to construct these sensors is a good illustration of an economical PCB MEMS process combined with a novel substrate, liquid crystal polymer, which is capable of manufacturing miniature low-cost sensors rapidly for aquatic applications. These sensors show potential for use in integrated MEMS systems for environmental measurements.

Acknowledgments

This work was supported by the Navy (grant number N00014-03-1-0480). The authors are grateful to Andres Cardenas, Carl Biver and George Steimle for their contributions on completing this project; Chad Lembke and Mark Holly for providing mechanical engineering support and David Edwards for providing the 3D surface topography measurements. Technical support from Joe Kolesar, Charles Jones and Nghia Huynh are gratefully acknowledged.

References

[1] Merkel T, Graber M and Pagel L 1999 A new technology for fluidic microsystems based on PCB technology *Sensors Actuators* A **77** 98–105
[2] Jayaraj K and Farrell B 1998 Liquid crystal polymers and their role in electronic packaging *Adv. Microelectron.* **25** 15–8
[3] Culbertson E 1995 A new laminate material for high performance PCBs: liquid crystal polymer copper clad films *45th Electronic Components and Technology Conf.* pp 520–3
[4] Wang X, Engel J and Liu C 2003 Liquid crystal polymer (LCP) for MEMS: process and applications *J. Micromech. Microeng.* **13** 628–33
[5] Hand A 2001 Start-up company exploits maskless photolithography technique *Sem. Int.* **24** 44
[6] Madou M 1997 *Fundamentals of Microfabrication* (Boca Raton, FL: CRC Press) pp 1–50
[7] Clescerl C, Greenberg A and Eaton A (ed) 1999 *Standard Method for the Examination of Water and Wastewater* 20th edn (Washington, DC: American Public Health Association)
[8] Hooker S and Boyd L 2003 Salinity sensors on seals: use of marine predators to carry CTD data loggers *Deep-Sea Res.* I **50** 927–39
[9] Sturlaugsson J and Gudbjornsson S 1997 Tracking of Atlantic salmon (*Salmo salar* L.) and sea trout (*Salmo trutta* L.) with Icelandic data storage tags *NOAA Technical Memorandum* National Marine Fisheries Service (San Diego, CA) NOAA-TM-NMFS-SWFSC-236 pp 52–54
[10] Downing J, McCoy K and DeRoos B 1992 Autonomous expendable CTD profiler *Sea Technol.* (September) 49–55
[11] Farruggia G and Fraser A 1984 *Miniature Towed Oceanographic Conductivity Apparatus Oceans 84 (Washington, DC, 10–12 September)*
[12] Norlin P, Ohman O, Ekstrom B and Forssen L 1998 A chemical micro analysis system for the measurement of pressure, flow rate, conductivity, UV-absorption and fluorescence *Sensors Actuators* **49** 34–9
[13] Wang X, Lu L and Liu C 2001 Micromachining techniques for liquid crystal polymer *14th IEEE Int. Conf. on Micro Electro Mechanical Systems, MEMS* pp 126–30
[14] Fries C, Fries D, Broadbent H, Steimle G, Kaltenbacher E and Sassarath J 2003 Direct write patterning of microchannels *1st Int. Conf. on Microchannels and Minichannels (Rochester, NY, USA, 24–25 April)*

[15] Gileadi E, Kirowa-Eisner E and Penciner J 1975 *Interfacial Electrochemistry: An Experimental Approach* (Reading, MA: Addison-Wesley) pp 216–8
[16] Jacobs P, Suls J and Sansen W 1990 A planar conductometric sensor showing excellent polarization impedance characteristics *Annu. Int. Conf. IEEE Eng. Med. Biol. Soc.* **12** 1484–5
[17] Lewis E 1980 The practical salinity scale 1978 and its antecedents *IEEE J. Oceanic Eng.* **5** 3–8